MANTLE HELIUM IN SOUTHERN QUEBEC GROUNDWATER: A POSSIBLE FOSSIL RECORD OF THE NEW ENGLAND HOTSPOT

Pauline MÉJEAN[1], Daniele L. PINTI[2], Takanori KAGOSHIMA[3], Emilie ROULLEAU[4], Laura DEMARETS[2,5], André POIRIER[2], Naoto TAKAHATA[3], Yuji SANO[2], Marie LAROCQUE[2]

1 - Laboratoire des Geosciences Environnement Toulouse (GET) and Observatoire Midi-Pyrénnées (OMP), 14 avenue Edouard Belin, 31400 Toulouse, France

2 - GEOTOP and Département des sciences de la Terre et de l'atmosphère, Université du Québec à Montréal, CP888, Succ. Centre-Ville, Montréal, QC, H3C 3P8, Canada

3 - Atmosphere and Ocean Research Institute, The University of Tokyo, Kashiwa, Chiba 277-8564, Japan

4 - STRATAGEM974, 62 boulevard du Chaudron, 97490 Ste Clotilde, La Réunion, France

5 - Centre Universitaire de Formation en Environnement et développement durable (CUFE), Université de Sherbrooke, Longueuil, QC, J4K 0A8, Canada

Keywords: noble gases; helium isotopes; groundwater; magma aging; Monteregian Hills; New England hotspot.

Abstract

The Monteregian Hills are an alignment of magmatic intrusions of Cretaceous age located in the St. Lawrence Lowlands, Quebec, Canada. Their origin is controversial and numerous studies have failed to decipher between a hotspot trail or sub-continental magmatism related to the opening of the North Atlantic Ocean. Here, we show that 17.7±9.6 % of the helium of the modern to Holocene-aged groundwater from the regional aquifer is of mantle origin, with a $^{3}He/^{4}He$ (R) of up to 1.42 times the atmospheric ratio (Ra). It suggests that a fossil Monteregian Hills magmatic signal, diluted by local radiogenic helium and preserved in the Monteregian Hills intrusions, is leached locally by flowing modern or sub-modern groundwater. Helium isotopic measurements by pyrolysis in Monteregian Hills bulk rocks and clinopyroxene separates show R/Ra values of up to 4.96, suggesting that fossil mantle helium has been partially preserved in these rocks and their mineral phases. Monte Carlo simulations of a magma aging model shows that the initial $^{3}He/^{4}He$ ratio in these Cretaceous intrusions could have been between 21±10Ra and 33±28Ra (2σ), favoring the hypothesis that the Monteregian Hills are the product of the passage of the North American plate over the New England hotspot. This study raises the prospect of using modern groundwater as an archive of mantle He over a hundreds of millions of years timescale.

1. Introduction

The Cretaceous Monteregian Hills Igneous Province is a WNW-ESE alignment of nine alkaline intrusions outcropping across the St. Lawrence Lowlands, Quebec, Eastern Canada (Fig. 1 and 2b). The magmatic source of these intrusions has been the subject of debate for nearly 40 years. Crough (1981) and later Sleep (1990) have suggested that the Monteregian Hills are the result of the passage of the North American plate over the New England hotspot (also called the Great Meteor hotspot), a long-lived hotspot presently overridden by the Mid-Atlantic Ridge, south of the Azores. However, numerous geochemical and isotopic investigations of Monteregian Hills rocks have failed to unequivocally indicate the presence of a plume source (e.g., McHone, 1996; Roulleau et al., 2012; Roulleau and Stevenson, 2013; Chen and Simonetti, 2015).

The helium isotope ratio, $^{3}He/^{4}He$ (R), can be used to trace the sources of continental magmatism. Indeed, the mantle is enriched in primordial isotope ^{3}He over radiogenic isotope ^{4}He when compared to the atmosphere (Ra = 1.382×10^{-6}: Sano et al., 2013). In continental settings, groundwater may contain helium derived from the mantle in regions of active transtensional deformation, even in regions where there is no substantial magmatism (e.g., Kennedy and van Soest, 1997). The processes that control the release of mantle-derived volatiles to the subsurface are likely sub-continental magma intrusions and underplating (Torgersen, 1993), with episodic advective transport in the crust (Castro, 2004). The occurrence of mantle helium should be identifiable in crustal environments, which are generally dominated by radiogenic ^{4}He, produced through the radioactive decay of U and Th contained in rocks, over ^{3}He, which can be produced only in minor amounts by neutron reactions with lithium (Tolstikhin et al., 1996). The resulting typical crustal $^{3}He/^{4}He$ ratio is 0.01-0.02Ra (Tolstikhin et al., 1996), distinctly lower than the ratio

expected for mantle-related fluids. The helium isotopic ratio of the convective mantle, as sampled in the mid-ocean ridge basalts (MORBs), is 8±1Ra (e.g., Allègre et al., 1995), while sub-continental lithospheric mantle (SCLM) has a lower ratio, 6.1±0.9Ra (Gautheron and Moreira, 2002).

The non-degassed lower mantle, the expected source of mantle plumes and their related products (Oceanic Island Basalts or OIBs), should have preserved a primordial, solar-type $^{3}He/^{4}He$ ratio, with R/Ra values greater than the MORBs value of 8±1 (e.g., Trieloff et al., 2000). However, measurements from OIBs show highly variable $^{3}He/^{4}He$ ratios. Some have higher $^{3}He/^{4}He$ than MORB values, up to 30Ra in Loihi seamount (Hawaii) (Kurz et al., 1982) and greater than 40Ra in NW Iceland (e.g., Harðardóttir et al., 2018), but several others have lower values than MORBs, such at Tristan de Cunha and Gough Islands (5-7Ra; Kurz et al., 1982). The highest R/Ra value reported so far is 49.5, measured in picrites from Baffin Island (Stuart et al., 2003). The reason for such high variability is still a matter of debate, and several hypotheses have been proposed, including: 1) ubiquitous air contamination during basalt eruption; 2) the addition of radiogenic helium from subducted plate components; 3) mixing between plume-derived material and material derived from the upper mantle; and 4) isotopic heterogeneity within the plume itself (e.g., Kurz et al., 1982; Graham, 2002).

Over the past 25 years, several studies have identified fossil mantle helium in groundwater from the eastern North American craton. In New Hampshire, Torgersen et al. (1995) identified the presence of helium with a substantial mantle fraction (≈ 12% of the total; $^{3}He/^{4}He$ = 1.2Ra) in modern groundwater from the Mirror Lake Basin aquifer, where there has been no volcanism since the Jurassic to Early Cretaceous (190-95 Ma ago). Torgersen et al. (1995) attributed this mantle helium to either the passage of the New England hotspot, which created the nearby White

Mountains magmatic province (Eby, 1985) or to magmatic episodes related to the closure of the Iapetus ocean (before 370 Ma). Castro et al. (2009) measured He and Ne in deep groundwater of the Michigan Basin revealing a primordial solar-like contribution. However, the absence of magmatism and of low-velocity seismic anomalies that would have indicated a fossil hotspot track in the region suggested that this primordial signature could be accounted for by a shallow refractory mantle reservoir underneath the Michigan Basin (Castro et al., 2009). Pinti et al. (2011) identified small amounts of mantle helium (2% of the total) in hundreds of millions of years-old brines located in the deeper sedimentary aquifers of the St. Lawrence Lowlands (BEC location in Fig. 1). Saby et al. (2016) also found mantle helium in the Ordovician-age regional aquifer of the Nicolet St-François watershed, St. Lawrence Lowlands (8% of the total; NSF location in Fig. 1).

Here, three new sets of helium isotopic data from groundwater and rocks collected from several locations in the St. Lawrence Lowlands are reported (Figs. 2a, 2b). The first set was measured in groundwater collected from sedimentary aquifers of the Vaudreuil-Soulanges watershed (Table 1), located west of Montreal, close to the Oka carbonatite complex (Fig. 2a). The second set of helium data was measured in groundwater circulating in the magmatic intrusions of the Monteregian Hills (Table 1 and Fig. 2b). The third was measured in Monteregian Hills bulk rocks and clinopyroxene separates, collected as part of a previous study (Roulleau and Stevenson, 2013; Fig. 2b). Measured $^{3}He/^{4}He$ ratios in both groundwater and rocks suggest the presence of a fossil helium magmatic signal diluted by local radiogenic helium, preserved in the Monteregian intrusions and leached locally by flowing modern to Quaternary-age groundwater. The initial helium signature of the magmatic source, before radiogenic dilution, is estimated here using Monte Carlo simulations of a magma aging model (Torgersen and Jenkins, 1982). The results bring new

and independent evidence of the past presence of a primitive plume beneath the region, which generated the Monteregian intrusions.

2. Geological background

2.1 Hydrology of sampled waters

The first set of groundwater samples was collected 10 km south of the Oka complex, in the Vaudreuil-Soulanges watershed (Table 1 and Fig. 2a). With a surface area of 814 km^2, Vaudreuil-Soulanges is the westernmost watershed of the St. Lawrence Lowlands basin (Fig. 2a). It consists of Cambrian fluvio-marine quarzitic sandstones of the Potsdam Group and Early Ordovician shelf-carbonates and dolostones of the Beekmantown Group unconformably overlying the granite-gneiss-anorthosite basement of the Mesoproterozoic (1250-980 Ma) Grenville Orogeny (Larocque et al., 2015). This sedimentary sequence constitutes the bedrock aquifer sampled in this study, and is covered by a 120 m-thick sequence of Quaternary glacial till and clays from the marine transgression episode of the Champlain Sea, which occurred between 12 and 9 ka ago.

The sedimentary sequence of the Vaudreuil-Soulanges watershed is disturbed by two main magmatic episodes: (1) the intrusion of the syeno-granitic body of Mont Rigaud, with a U-Pb age of 564^{+10}_{-8} Ma (Malka et al., 2000); and 2) K-rich alnoïtes intruding the sedimentary cover in the central-eastern part of the watershed at the location of Île Cadieux, with ages ranging 108 to 113 Ma (Fig. 2a; Eby, 1987; Chen and Simonetti, 2013). Although only the latter intrusion outcrops in the watershed, a regional low-resolution aeromagnetic survey of the St. Lawrence Lowlands has shown that hundreds of smaller intrusions lie under the sedimentary cover, with a high magnetic

alignment corresponding to the northern region of the Vaudreuil-Soulanges watershed (see maps at http://www.mrnfp.gouv.qc.ca/produits-services/mines.jsp). Several of these intrusions outcrop in numerous quarries, or reach the surface, by crosscutting the Ordovician sedimentary sequences of the St. Lawrence Lowlands (e.g., Harnois et al., 1990; Harnois and Mineau, 1991).

Recharge of the Cambrian-Ordovician bedrock aquifer is mainly from high-permeability Quaternary eskers and sand hills, which crosscut the low-permeability glacial till and the Champlain Sea clays. Less recharge is from the higher topography zone, corresponding to the Mont Rigaud syenitic intrusion. Regional groundwater flows from these topographic highs to the Ottawa River in the northern part of the area, and S-SE, in the direction of St. Lawrence River and Lake Saint-Francois in the southern part of the basin (Fig. 2a). Méjean (2016) reported modelled ^{3}H-^{3}He groundwater ages to be from 8.5±0.6 a to 57±4 a, with several samples showing ^{3}H of 0.8 Tritium Units (TU; 1 TU is defined as the ratio of 1 tritium atom to 10^{18} hydrogen atoms), which corresponds to the environmental background, suggesting the presence of older water masses. This fossil water component was dated using the U-Th/^{4}He method to be older than 45 ka (Méjean, 2016).

The second set of groundwater samples was collected from wells tapping directly into the fractured intrusive rocks of the Monteregian Hills at St. Bruno, St. Hilaire, Rougemont, Yamaska, and Brome (Fig. 2b and Table 1). Little is known about groundwater circulation in the Monteregian Hills. Geophysics have revealed the presence of several buried dykes around these hills, but the consequences for groundwater circulation are still unknown. A recent study by Beaudry et al. (2018) revealed that the Monteregian Hills contain confined to semi-confined aquifers, with water ages between modern and 3-12 ka. Groundwater from the Monteregian Hills belongs to two

chemical groups (Beaudry et al., 2018): 1) Group "A1", which consists of modern recharge water associated with the presence of tritium, low salinity (Total Dissolved Salinity (TDS) of 168 mg/L), and a Ca-HCO_3 water type with relatively low pH (6.5) and a composition controlled by carbonate dissolution; and 2) group "A2", which consists of evolved Na-HCO_3 composition water with high pH (7.8) and slightly saline (TDS of 368 mg/L) due to mixing with brackish water of the Champlain Sea marine invasion (Beaudry et al., 2018).

2.2 The debated origin of the Monteregian Hills

The Monteregian Hills alkaline province consists of plutons, dikes, and sills that were emplaced along faults associated with the Ottawa-Bonnechere graben (Fig. 2). The intrusions were emplaced into the Cambro-Ordovician sediments of the St. Lawrence Lowlands and the folded and thrusted Lower Paleozoic sequence of the Appalachian orogen (Figs. 1 and 2b). Carbonatite and associated alkaline rocks occurr at the Oka complex, just north of the Vaudreuil-Soulanges watershed (Fig. 2a). Further east, the plutons are dominated by ultramafic and mafic rocks (gabbros) with fewer syenites. Toward the eastern end of the province, silica-saturated mafic and felsic rocks become dominant components of the plutons. Geochronological data from the Oka carbonatite complex by Chen and Simonetti (2013) show bimodal U-Pb ages centered on 113 Ma for alnöitic intrusions and 135 Ma for ijolite rocks. Measured $^{40}Ar/^{39}Ar$ ages of the other Monteregian complexes fall within the restricted range of 124±1 Ma (Foland et al., 1986).

The alkaline character of the Monteregian Hills and the Sr (0.7032–0.7040) and Nd (0.5125–0.5127) isotopic composition similar to those found in some OIBs supported a plume-related mantle source (Foland et al., 1986). McHone (1996) showed that there is no evidence of

age progression within and among the different magmatic provinces supposedly created by the New England hotspot (Monteregian Hills in Quebec, White Mountains in New England, and the New England seamounts off the east coast of the US), as would be expected of a hotspot track, arguing for the involvement of heterogeneous SCLM melts rather than plume material. A decrease in the buoyancy flux of the New England hotspot from the New England seamounts to the Monteregian Hills was estimated by Sleep (1990), who explained that the lack of an obvious track may be due to either the failure of the plume to penetrate the Canadian Shield. Roulleau et al. (2012) observed an inverse relationship between $^{206}Pb/^{204}Pb$ and $N_2/^{36}Ar$ ratios, interpreted as the mixing between a plume source with a recycled component (HIMU, High $\mu = {}^{238}U/^{204}Pb$) and an ambiguous mantle source that could be either a non-HIMU-type plume source (such as that feeding Loihi; Dixon and Clague, 2001) or the depleted mantle. Roulleau and Stevenson (2013) provided new isotopic data (Nd-Sr-Hf-Pb) suggesting a dominant lithospheric mantle source for the Monteregian Hills, but contaminated by rising asthenospheric mantle that progressively thermomechanically eroded the lithosphere, hence, producing a metasomatized lithospheric mantle with HIMU and EMI reservoirs. Finally, some other authors have ascribed the Monteregian magmatism to the melting of the lithospheric mantle through NW-SE Iapetus-related faults reactivated at the time of the North Atlantic Ocean opening (e.g., Faure et al., 1996).

3. Materials and analytical methods

3.1 Groundwater sampling

A total of 24 groundwater samples were collected from open bedrock municipal wells, domestic wells, and piezometers. Sixteen were sampled in the Cambrian-Ordovician fractured

bedrock aquifer of the Vaudreuil-Soulanges watershed in the summer of 2014, at depths ranging between 20 m and 96 m. A second set of eight groundwater samples was collected in the summer of 2016, from fractured aquifers of the Monteregian Hills: Mount St. Bruno, Mount St. Hilaire, Mount Rougemont, Mount Yamaska and Mount Brome (Fig. 2b and Table 1). After purging the well, water was collected in 3/8-inch diameter refrigeration-type copper tubes, which were then cold-sealed following the method described in Vautour et al. (2015). Helium isotopic ratios of groundwater samples collected in 2014 were measured at the University of Tokyo, using a VG Helix SFT and compared to the Helium Standard of Japan (HESJ; Matsuda et al., 2002), with a 2σ precision of ±1%. The ^{4}He and ^{20}Ne concentrations were measured on a Pfeiffer Prisma™ 80 quadrupole mass spectrometer connected to the purification line (see Vautour et al., 2015 for details).

The eight samples collected in 2016 were analyzed at the GEOTOP Noble Gas Laboratory. After extraction and purification on one Ti-sponge and two ST-707 getters, helium was cryogenically separated and released at 40K into a HELIX-MC (Thermo®) mass spectrometer, and ^{3}He/^{4}He ratios were measured by peak jumping on the axial CDD (^{3}He) and Faraday (^{4}He) detectors, with a precision of ca. 3% on the ^{3}He and less than 0.01% on ^{4}He, calibrated against an air pipette. Helium and neon elemental composition was measured in a Pfeiffer Prisma™ C-200 quadrupole mass spectrometer connected to the purification line, following the procedures described in Roulleau et al. (2012).

3.2 Bulk rocks and mineral separates

A total of nine rock samples (Figs. 2a, b) were collected from the Oka complex (OC; n=1), Île Cadieux (Aln, n=1), Mount Royal (MR; n=1), Mount St. Bruno (MSB, n=1), Mount Rougemont (MR, n=2), Mount Brome (MB, n=1), Mount St. Hilaire (MSH, n=1), and Mount Yamaska (MY, n=1). Pyroxene is among the first minerals to crystallize in the magma chamber, together with olivine, and thus documents the least evolved melt available. Monteregian Hills gabbros contain very small and few olivine crystals, so clinopyroxene remains the main phase to analyze (Sasada et al., 1997; Roulleau et al., 2012). Clinopyroxene grains were thus hand-picked from the Mount St. Bruno sample (SMB3-R; Table 2). Helium was extracted and analyzed at the University of Tokyo using a two-stage analytical process. Whole–rock samples and mineral separates (~0.5 g) were wrapped in 10 μm-thick aluminum foil and stored inside the glass part of an induction furnace under vacuum to degas weakly-bound atmospheric gases. Individual samples were then moved into a Mo-Ta furnace and pyrolyzed at 1800˚C for 30 mn (Kagoshima et al. 2012). The gas was purified, cryogenically separated, and He contents were determined on a Pfeiffer QMS Prisma™ quadrupole mass spectrometer connected to the vaccum purification line. The $^{3}He/^{4}He$ ratios were measured using the HELIX-SFT mass spectrometer (R-OC and R-Aln) and the VG5400 mass spectrometer (R-MR15, R-MSB3, R-MB15, R-MRg1, R-MRg9, R-MSH1, R-MY3) following the procedures described above.

The rock samples collected in the Vaudreuil-Soulanges and the Monteregian Hills areas were analyzed by Bureau Veritas® laboratories in Vancouver for trace elements, including U and Th, reported in Table 2. Samples were finely crushed and mixed with $LiBO_2/Li_2B_4O_7$ flux. Crucibles were fused in a furnace. The cooled bead was dissolved in ACS grade nitric acid and

trace elements were analyzed using two different instruments: Elan 9000 ICP-MS and Spectro Ciros Vision ICP-ES. Loss on ignition (LOI) was determined by igniting a sample split then measuring the weight loss. The detection limits for U and Th by ICP-MS are 0.1 and 0.2 ppm respectively.

4. Results

The atmosphere-normalized $^{3}He/^{4}He$ ratios (R/Ra) of the groundwater samples range from 0.15±0.01 to 3.32±0.08, pointing to the presence of both ^{3}He-enriched and ^{4}He-enriched sources (Table 1). Dissolved ^{4}He concentrations vary over three orders of magnitude. The lowest helium concentration is 6.64 x 10^{-8} $cm^{3}STP/g_{H2O}$ (VS104), which is slightly higher than the value expected from solubility equilibrium with the atmosphere (Air Saturated Water or ASW) at 9.8°C, of 4.7 x 10^{-8} $cm^{3}STP/g_{H2O}$, which represents helium contained in freshwater at recharge. Two samples show very high ^{4}He concentrations: Mount St. Hilaire (WMSH3), with ^{4}He of 0.0786 $cm^{3}STP/g_{H2O}$, and Mount Brome (WMB8), with ^{4}He of 1.27 x 10^{-4} $cm^{3}STP/g_{H2O}$. These high ^{4}He concentrations are also accompanied by high ^{20}Ne concentrations. In the case of WMSH3, the high $^{4}He/^{20}Ne$ of 49.80 excludes the presence of excess air and the contemporary He-Ne enrichment could be related to bubbling and a bi-phase (gas-water) mixture not sampled at the solubility equilibrium, as observed in a few wells in the St. Lawrence Lowlands (Vautour et al., 2015). The ^{4}He concentrations have been corrected assuming a ^{20}Ne content at solubility equilibrium of 9.3 x 10^{-7} and 1.65 x 10^{-8} $cm^{3}STP/g_{H2O}$ for WSMH3 and WMB8, respectively. Sample WMSH3 also shows the lowest and most radiogenic $^{3}He/^{4}He$ ratio, of 0.15±0.01, which is caused by the high U and Th contents in this

Monteregian intrusion. Mount St. Hilaire is indeed known for its high natural radioactivity, which produces high ^{222}Rn concentrations in groundwater (234 Bq/L; Pinti et al., 2014).

The $^{3}He/^{4}He$ ratios measured in the bulk rocks range from 0.06±0.02 (R-Aln) to 1.36±0.11Ra (R-Mrg9). Higher values were obtained in the clinopyroxene separated from sample R-MSB3, with R/Ra = 1.23±0.10 and 4.96±0.01. The total amount of ^{4}He measured ranges from 7.90 x 10^{-7} $cm^{3}STP/g_{rock}$ to 2.28 x 10^{-5} $cm^{3}STP/g_{rock}$ (Table 2). The measured $^{3}He/^{4}He$ ratios in mineral separates is similar to, or higher than, those measured by Sasada et al. (1997) in Oka intrusion diopside, of 0.25±0.07 and 2.55±0.25Ra (Table 2).

5. Discussion

5.1 Helium sources in Vaudreuil-Soulanges and Monteregian Hills groundwater

Helium dissolved in groundwater can have multiple sources. Each helium component must be correctly identified in order to determine the mantle-derived one, if any. In groundwater, the helium components are:

$$^{3}He_{tot} = {}^{3}He_{eq}+{}^{3}He_{tri}+{}^{3}He_{ea}+{}^{3}He_{rad}+{}^{3}He_{mtl} \qquad (1) \text{ and}$$

$$^{4}He_{tot} = {}^{4}He_{eq}+{}^{4}He_{ea}+{}^{4}He_{rad}+{}^{4}He_{mtl} \qquad (2),$$

where the suffix “eq” indicates atmospheric helium dissolved in groundwater during recharge at solubility equilibrium (ASW); “ea” is the excess-air helium resulting from air bubbles entering the water table at recharge and dissolving into groundwater (Heaton and Vogel, 1981); “tri” is the ^{3}He

produced by the decay of atmospheric tritium dissolved in water, commonly referred to as tritiogenic helium; "mtl" is the mantle helium; and "rad" is the radiogenic helium produced in the aquifer. The latter can produce ^{3}He from neutron reactions on lithium ($^{6}Li(n,\alpha)^{3}H(\beta)^{3}He$) and ^{4}He are the α-particles supplied through the decay of $^{235,238}U$ and ^{232}Th and their decay products (Andrews and Kay, 1982). Radiogenic and mantle helium are commonly grouped using the term "terrigenic".

There is another potential source of ^{3}He, which is often ignored: cosmogenic ^{3}He produced by spallation reactions between cosmic ray neutrons and the major elements of the rock. Cosmogenic ^{3}He is produced in rocks in the uppermost 1 m of Earth's surface and could potentially be transferred to groundwater. However, calculations from Marty et al. (1993) of potential cosmogenic ^{3}He in groundwater of the Paris Basin have shown that cosmogenic production in rocks is very limited as a potential source, and cannot account for significant ^{3}He anomalies in groundwater. Sediments from Vaudreuil-Soulanges watershed outcropped in Ordovician time (430 Ma ago), but were then rapidly buried for several hundred million years, so that any cosmogenic ^{3}He produced is expected to have been completely diluted by continuous radiogenic ^{4}He production, and thus not detectable in our samples.

A convenient graphical approach to separate the different helium components is to plot the $^{3}He/^{4}He$ ratio corrected for the excess-air component ($[^{3}He_{tot}-^{3}He_{ea}]/[^{4}He_{tot}-^{4}He_{ea}]$) against the ratio of ASW helium (He_{eq}) to total helium, corrected for the excess-air component ($^{4}He_{eq}/^{4}He_{tot}-^{4}He_{ea}$) (Weise and Moser, 1987). In our samples, the excess air component is calculated as the difference between the expected ASW value of ^{20}Ne at the well temperature and the measured one.

In this diagram, which is commonly referred to as a "Weise plot" (Fig. 4a), helium of purely atmospheric origin (ASW composition) plots on the coordinates ([$^3He_{tot}$-$^3He_{ea}$]/[$^4He_{tot}$-$^4He_{ea}$]) or R_{eq} = 1.36 x 10^{-6} (0.983Ra; Benson and Krause, 1980) and ($^4He_{eq}$/$^4He_{tot}$-$^4He_{ea}$) = 1 respectively (Fig. 4a). If only tritiogenic $^3He_{tri}$ is added to an initial atmospheric composition, then the sample composition will plot parallel to the right Y-axis, starting from the initial ASW composition (Fig. 4a). If radiogenic ^3He, produced through neutron reactions with ^6Li, and ^4He, produced through the α-decay of $^{235,238}U$ and ^{232}Th, are added, the initial ASW composition will shift closer to the bottom-left corner of the plot (R_{rad}; Fig. 4a). In the St. Lawrence Lowlands fractured bedrock, the crustal R_{rad} is calculated to be 1.66 x 10^{-6} (0.012Ra), based on Li, U, and Th contents measured from 398 rocks of the region (Pinti et al., 2011). Finally, if mantle-derived helium is present, sample composition will plot parallel to the Y-axis, starting from a radiogenic crustal composition (R_{terr}; Fig. 4a).

On the Weise plot, mixing between helium components appears as straight lines governed by the equation (Weise and Moser, 1987; Fig. 4a):

$$\underbrace{\frac{\left({}^3He_{tot}-{}^3He_{ea}\right)}{\left({}^4He_{tot}-{}^4He_{ea}\right)}}_{Y}=\underbrace{\left(R_{eq}-\mathrm{R}_{terr}+\frac{{}^3He_{tri}}{{}^4He_{eq}}\right)}_{m}\cdot\underbrace{\frac{{}^4He_{eq}}{{}^4He_{tot}-{}^4He_{ea}}}_{X}+\underbrace{R_{terr}}_{b} \qquad (3),$$

where R_{terr} is the $^3He/^4He$ of the terrigenic source, which corresponds to either crustal helium, mantle-derived helium, or both.

Groundwater samples from Vaudreuil-Soulanges and the Monteregian Hills align along mixing lines representing the complete decay of 6.7TU, 14.5TU, 18.5TU, 40TU, 61TU, and 285TU, and a terrigenic end-member, R_{terr}, with values between 0.16Ra and 1.48Ra ($^3He/^4He$ values

between 2.2 x 10^{-7} and 2.05 x 10^{-6}; Fig. 4b). These ratios are higher than those expected from the local production of ^{3}He from ^{6}Li and of ^{4}He from $^{238,235}U$ and ^{232}Th in St. Lawrence Lowlands sedimentary rocks or in rocks from the Grenville basement, of 0.45 to 1.66 x 10^{-8} (Pinti et al., 2011). The difference between the expected crustal R_{rad} and the maximum calculated R_{terr} from the Weise plot (i.e., the intercept of the mixing line between samples WSB1, WSB2, and WY6; Fig. 4b) suggests the addition of 18.4±6.7% of mantle-derived helium (labelled "f_{mtl}" in Fig. 4b). The total uncertainty on the value comes mainly from the error on the intercept of the regression. Uncertainty derived from the variability of the mantle end-member helium isotopic ratio (8±1) and the possible variability on the crustal ratio (0.01 to 0.1Ra; Tolstikhin et al., 1996) produces less than 2% error. It is worth noting that here a $^{3}He/^{4}He$ mantle end-member ratio of 8±1 is assumed for sake of consistency with previous estimates from Pinti et al. (2011) and Saby et al. (2016). If the closer mixing line between samples VS-105-2, VS-108-2, and VS-108-2 and the sample from Mount Rougemont (WR-5) is taken, the intercept will give a R_{terr} of 1.86 x 10^{-6} (or 1.35Ra; Fig. 4b). This is equivalent to a mantle fraction of 16.7±6.9%. This value is, within uncertainty, similar to the previous estimate.

These two f_{mtl} values represent the highest mantle helium fractions ever reported for St. Lawrence Lowlands groundwater, higher than the 2% and 8% calculated by Pinti et al. (2011) and Saby et al. (2016), respectively. However, the calculated mantle He fractions could be conservative minimal estimates. The complete decay of 1TU in a gram of water corresponds to 2.49 x 10^{-15} $cm^{3}STP/g_{water}$ of ^{3}He. Assuming an initial $^{4}He_{ASW}$ of 4.72 x 10^{-8} $cm^{3}STP/g_{water}$, corresponding to the dissolution of atmospheric helium at 9.8˚C, which is the average temperature of the groundwater in the region (Vautour et al., 2015), the corresponding $^{3}He_{ASW}$ would be 6.42 x 10^{-14} $cm^{3}STP/g_{water}$.

Adding 285TU of tritium would produce a tritiogenic $^{3}He/^{4}He$ ratio of 11.86Ra. This value is not unreasonable for aquifers that contain a mixture of modern and older water, but is actually more than double the highest tritiogenic $^{3}He/^{4}He$ ratio measured among the 125 groundwater samples from Bécancour and Nicolet-St. François watersheds (internal compilation of unpublished data), and equal to 4.59±0.03Ra (equivalent to the decay of 94.5TU). If the maximum amount of tritium preserved in groundwater of the St. Lawrence Lowlands aquifers is 94.5TU, then the mixing line passing through, e.g., sample WSB1 (mixing line reported as an example in Fig. 4a), will have an intercept (R_{terr}) at $^{3}He/^{4}He = 4.28 \times 10^{-6}$, which is equivalent to the addition of 38.6% of mantle helium. For the purpose of this study and the following modeling, the average value of the two f_{mtl} estimates above (18.4±6.7% and 16.7±6.9%), i.e. 17.7±9.6% (equivalent to a $^{3}He/^{4}He$ ratio of 1.42±0.14Ra), is assumed here (orange star in Fig. 4b).

5.2 Origin of terrigenic helium in Vaudreuil-Soulanges and Monteregian Hills groundwater

The ^{3}He in excess of crustal production (Fig. 4b) can be explained by the presence of a mantle helium component in groundwater of the Vaudreuil-Soulanges watershed and in the Monteregian Hills local aquifers. The preservation of this mantle component in groundwater could be explained by 1) mantle He concentrated at the base of the crust and migrating through crustal-rooted faults; 2) a fossil mantle source preserved in very old brines having ages contemporary with the emplacement of the Monteregian Hills intrusions; or 3) a fossil mantle signal preserved in Monteregian Hills magmatic intrusions, but released in recent groundwater by water-rock processes, such as mineral dissolution or diffusive exchange.

The first hypothesis can be discarded. For example, Lee et al. (2019) have shown that mantle He can reach shallow groundwater through active strike-slip faults. Fluids are thought to enhance pore fluid pressures in association with fault weakening caused by seismicity. This will facilitate the upward migration of deep-seated helium. Although Quebec is the second more seismic area in Canada, seismicity seems to be caused by residual friction provoked along fault planes by the crustal isostatic rebound following the last deglaciation (Lamontagne, 2002). Fission-track and U-Th/He thermochronology of the Cambrian St-Lawrence Lowlands Rift Zone showed that fault activity in the region continued until the Mesozoic and terminated in the Cretaceous (Tremblay et al., 2013). Consequently, it is difficult to assume that present-day micro-seismicity has weakened these old tectonic structures to facilitate the upward migration of mantle helium in the region.

If the second hypothesis is valid, then old groundwater of at least the age of the Monteregian Hills intrusions (124±1 Ma) should have been preserved in the study area. Pinti et al. (2011) found brines with possible Mesozoic ages in the Cambro-Ordovician aquifers of the Potsdam Group of the St. Lawrence Lowlands supergroup in the Bécancour area (Fig. 1). However, these brines have little mantle-derived ^{3}He (2% of the total), are highly saline Ca-Na-Cl type (up to 315,000 mg/L) waters, and are very radiogenic ($^{87}Sr/^{86}Sr$ of 0.71214), characteristic of Precambrian basement brines. Groundwater from Vaudreuil-Soulanges and from Monteregian Hills aquifers are of Ca-HCO_3 or Na-HCO_3 types, with very low salinity (168-710 mg/L), mainly derived from exchange with glacio-marine porewater from the Champlain Sea clays (Larocque et al., 2015; Beaudry et al., 2018). The presence of tritium in several Vaudreuil-Soulanges groundwater samples suggests modern water, possibly mixed with Holocene to Quaternary glacial water containing predominantly radiogenic ^{4}He, as suggested by Méjean (2016). Similar ages, from modern to 13

ka old, have been proposed for Monteregian Hills groundwater (Beaudry et al., 2018). Therefore, the occurrence of Mesozoic brines in the Vaudreuil-Soulanges and Monteregian Hills aquifers appears to be unlikely.

The third alternative and most plausible explanation, which will be explored in detail in the following sections, is the presence of a fossil mantle source, diluted over time through the addition of local radiogenic ^{4}He (the so-called "magma aging model"; Torgersen and Jenkins, 1982), preserved in magmatic intrusions, and recently released into groundwater through leaching.

5.3 Impact of in situ helium production on the "magma aging" model

The ^{3}He production in the crust is controlled by the thermal neutron capture of ^{6}Li in the reaction $^{6}Li(n,\alpha)^{3}H(\beta^{-})^{3}He$ (Andrews and Kay, 1982), while ^{4}He production is regulated by the α-decay of ^{238}U, ^{235}U, and ^{232}Th. In this study, the nucleogenic production rate of ^{3}He was calculated based on the Li abundances reported by Pinti et al. (2011) and Gold (1966) for the main Monteregian Hills lithologies. These vary from 11 ppm for a pyroxenite to 28 ppm for a gabbro (representing the lithologies of samples R-MSB3, R-MB15, R-MRg1, R-MRg9, R-MSH10, and R-MY3), 37 ppm in diorite (sample R-MR-15), and 15 ppm in carbonatite and in alnoïte. U and Th concentrations have been measured in bulk rocks and range from 3.3 to 12.4 ppm and from 9.4 to 40.9 ppm respectively (Table 2; data from this study and Roulleau and Stevenson, 2013). Li, U, and Th concentrations were not measurable in mineral separates.

The ^{3}He production rate for Monteregian Hills bulk rocks was calculated using the modified equation of Castro (2004):

$$J_{3He} = (2.69 \times 10^{-4}[U] + 6.40 \times 10^{-5}[Th]) \times [Li] \times 10^{-23} \times 22414 \qquad (4),$$

where J^3He is the ^3He production rate in $cm^3STP/g_{rock}/yr$; [U], [Th] and [Li] are the U, Th and Li concentrations in ppm. The ^3He production rate varies from 0.63 x 10^{-20} $cm^3STP/g_{rock}/yr$ in the Oka carbonatite to 2.89 x 10^{-20} $cm^3STP/g_{rock}/yr$ in Mont Brome gabbro (Table 2).

The ^4He production rate (J_{4He} in $cm^3STP/g_{rock}/yr$) is calculated following the equation (Torgersen et al., 1995):

$$J_{4He} = (0.2355 \times 10^{-12}) \times [U] \times \left(1 + 0.123\left(\frac{[Th]}{[U]} - 4\right)\right) \qquad (5),$$

where [U] and [Th] are the concentrations of U and Th in the rock in ppm (Table 2). The ^4He production rate varies from 0.63 x 10^{-13} $cm^3STP/g_{rock}/yr$ in the Oka carbonatite and Mount Royal gabbro to 2.07 x 10^{-12} $cm^3STP/grock/yr$ in Mount Brome gabbro (Table 2). The resulting $^3He/^4He$ derived by the *in situ* production of helium isotopes in rocks ranges from 0.005 to 0.0013 (Table 2), well below the values measured in fluids, confirming that the groundwater contains a fraction of terrigenic helium derived from a mantle reservoir (Table 1).

5.4. Monte Carlo simulation of a helium magma aging model

To test whether the high terrigenic $^3He/^4He$ ratios measured in groundwater (Table 1 and Fig. 4b) could reflect the presence of a fossil mantle source, diluted over time by the addition of *in situ*-produced radiogenic ^4He, a "magma aging" model is developed here (Torgersen and Jenkins, 1982). This model describes the evolution of an initial magmatic $^3He/^4He$ ratio in a magma body since its crystallization, by the addition of radiogenic ^4He produced *in situ* by ^{235}U, ^{238}U, and ^{232}Th α-decay (Torgersen and Jenkins, 1982). Consequently, the U and Th amounts in the magma source

determine the rate of change of the helium concentration of the rock, while the initial concentration of helium in an emplaced magma determines the change in the isotope ratio of helium (R_{mtl}/Ra). The model does not take the nucleogenic production of ^3He from Li into account, which is considered here to be negligible.

The initial $^3He/^4He$ ratio in the magma source (R_{mtl}/Ra) can be calculated following the equation:

$$\left(\frac{R_{mtl}}{Ra}\right)_{initial} = \frac{\left[\left(\frac{R_{mtl}}{Ra}\right)_{final} \times \left({}^4He_{initial} + J_{4He} \times t\right)\right]}{{}^4He_{initial}} \qquad (6),$$

where $(R_{mtl}/Ra)_{final}$ is the $^3He/^4He$ ratio measured in modern groundwater and normalized to the air value; $^4He_{initial}$ is the amount of ^4He in the magma source at t=0; J_{He} is the radiogenic ^4He production rate as calculated from eqn. (5); and t is the time since the magma emplacement.

From the results plotted on the Weise diagram, an average $(R_{mtl}/Ra)_{final}$ value of 1.42±0.14 Ra is assumed, equivalent to a mantle fraction f_{mtl} of 17.7±9.6% (orange star in Fig. 4b). Time, t, is assumed to be equal to the average age of alnoïte in Vaudreuil-Soulanges (110.5±3.5Ma), which ranges from 108±1Ma and 113±1Ma (Eby, 1985; Chen and Simonetti, 2013) and of the Monteregian Hills magmatic bodies (124±1 Ma; Foland et al., 1986). The J_{4He} for the alnoïte is 8.41 x 10^{-13} $cm^3STP/g_{rock}/yr$. An uncertainty of 20% is assumed, based on the variability of trace elements measured in alnöite from Île Cadieux by Harnois and Mineau (1991). The J_{4He} calculated for the Monteregian Hills is highly variable, depending on the U and Th contents in different lithologies, from gabbro to syenite (Table 2). Here, an average J_{4He} of 11.78±5.01 x 10^{-13} $cm^3STP/g_{rock}/yr$ is assumed.

A critical parameter to determine is the $^4He_{initial}$. In the magma aging model to explain mantle helium anomalies in groundwater of the Eastern America margin, Torgersen et al. (1995) suggested the value of 6.7 x 10^{-6} cm^3STP/g_{rock}. This value would best represent a gas-rich magma that has retained significant volatiles. The highest ^4He concentration in OIBs glasses (database from Graham et al., 2002; n=107) is of 6.24 x 10^{-6} cm^3STP/g_{rock}, very close to the theoretical value of Torgersen et al. (1995). Torgersen et al. (1995) considered this concentration to be a good proxy for a hot spot source. Indeed plume-derived melts should represent the non-degassed lower mantle, which is expected to have preserved more volatiles than the upper degassed mantle, in the canonical view of an Earth' mantle layered reservoir based on noble gas systematics (e.g., Allègre et al., 1995). However, OIBs are constantly depleted in helium compared to the MORBs (e.g., Moreira and Kurz, 2013). This contradiction is known as the "mantle helium paradox" (e.g., Hopp and Trieloff, 2008). There are several models to explain this paradox (e.g., Hopp and Trieloff, 2008; Gonnermann and Mukhopadhyay, 2007) but basically it is assumed that plume melts undergone a non-equilibrium degassing elemental fractionation during their ascent to the surface (Gonnermann and Mukhopadhyay, 2007). This model is based on the effect of CO_2 and H_2O contents in the melts which can drastically reduce the solubility of noble gases. OIB melts would be enriched in CO_2 compared to MORB ones, decreasing substantially the solubility of He which will tend to be largely degassed. Gonnermann and Mukhopadhyday (2007) constrained the He content in the pre-degassed melt to be 3 x 10^{-4} cm^3/g_{rock}, suggesting that more than 99 % of helium is lost during non-equilibrium magmatic degassing. This ^4He content is 2 orders of magnitude higher than that expected for the MORB magma source (3±2 x 10^{-6} cm^3STP/g_{rock}; Moreira and Kurz, 2013).

All parameters of Eqn. (6) with assumed or measured uncertainties are summarized in Table 3. An alternative way to calculate $^{4}He_{initial}$ is from rock analyses (Table 2). However, this is limited by the diffusion and loss of He from the rocks and the distribution of U and Th in the rock matrix and its effect on the dilution of the mantle signal, which is likely preserved in U and Th-poor minerals, such as in clinopyroxene.

The initial $^{3}He/^{4}He$ ratio expected in the fossil gas-rich magma source in the region ($R_{mtl}/Ra_{initial}$; Eqn. (6)) has been evaluated, together with its total uncertainty, using a Monte Carlo simulation. Monte Carlo simulations make use of the uncertainty domains for all given variables (Table 3) in a specific model, here the magma aging model explicated in Eqn. (6). By running the algorithm multiple times –a hundred thousand times here – with random sampling of those variables, individual output data can be generated. The probability distribution of the outputs is usually reported as a Gaussian curve, and the average and standard deviation thereof can be extrapolated.

Monte Carlo simulations were carried out using the NIST Uncertainty Machine (https://uncertainty.nist.gov/), which is a web-based software application to evaluate the measurement uncertainty associated with an output quantity defined by a measurement model of the form $y = f(x1,...,xn)$ (Lafarge and Possolo, 2015). Input parameters (Table 3) are introduced online, the number of iterations is selected, and the measurement model (Eqn. 6) is compiled in an "R" script.

Two simulations were carried out, representing two extreme cases (Table 3). The first one considers the progressive aging of a magma source equal to the alnöite, which emplaced between 107 and 114 Ma ago. The second one considers the progressive aging of an average magma source

of gabbro-sienitic composition, equal to the intrusions of the Monteregian Hills and emplaced 124±1Ma ago. A $^4He_{initial}$ content of 6.7±(10%) x 10^{-6} cm^3STP/g_{rock} is assumed, equivalent to the least degassed OIBs. We could consider an even more degassed OIBs source, however, for $^4He_{initial}$ contents ≤ 10^{-7} cm^3STP/g_{rock}, the initial helium isotopic ratios would be rapidly diluted by *in situ* radiogenic ^4He production on a timescale of 10Ma or even less, completely masking any mantle helium record in present-day volcanics.

The outputs of the Monte Carlo simulations have been represented in two different ways. The first, reported in Fig. 5 is as the resulting Gaussian curves for alnöite and for the Monteregian Hills intrusions (MH) simulations. The first simulation for the alnöite resulted in a $R_{mtl}/Ra_{initial}$ of 21±10 (2σ), while that for the gabbro-sienitic MH resulted in a $R_{mtl}/Ra_{initial}$ of 33±28 (2σ). The larger uncertainty for the second simulation is due to the larger error assumed on the J_{4He} (Eqn. 5 and Table 2) parameter. The output probability distributions for the two simulations have been compared with the frequency histogram of the measured $^3He/^4He$ ratios in 401 samples of OIB glasses (Fig. 5). The latter data was extracted from the global dataset of noble gas abundances and isotopic ratios in Volcanic Systems – USGS-NoGaDat, compiled by Abedini et al. (2006). Present-day plume-sourced helium in OIB glass phase has an average R/Ra of 15.8±8.6 (1σ) (Fig. 5).

Results of the Monte Carlo simulations have also been reported in a clearer way (Fig. 6), where the progressive "aging" of the initial helium isotopic signature of the emplaced magma to the present-day measured value is reported as a curve, together with its uncertainty envelope calculated from the Monte Carlo simulations. For the two simulations, up to 96% of the results show $(R_{mtl}/Ra)_{initial}$ higher than that expected for a lithospheric magma source, either the convective upper mantle (R=8±1Ra; Allègre et al., 1995) or the SCLM (R/Ra=6.1±0.9; Gautheron and

Moreira, 2002) (Fig. 6a). In this simulation, the mantle $^{3}He/^{4}He$ ratio is assumed to have been constant in the last 120Ma, which is what is expected from numerical simulations of the helium isotopic evolution in mantle reservoirs (e.g., Porcelli and Elliot, 2008).

These two simulations suggest that a mantle plume was possibly the source of the fossil helium presently found in the groundwater of the southern Quebec, which may be related to the New England hotspot.

If the previous Monte Carlo simulations were carried out using an undegassed OIB source $^{4}He_{initial}$ content of 3.14±(10%) x 10^{-4} $cm^{3}STP/g_{rock}$ (Gonnermann and Mukhopadhyday, 2007), then the resulting $(R_{mtl}/Ra)_{initial}$ will be very low from 1.8±0.2Ra (alnoïte) to 2.4±0.4Ra (Monteregian Hills). These values are even lower than those expected for a MORB or the SCLM-type magma source. Further, it would be very difficult to explain how the plume-generated melts beneath the Monteregian Hills could have preserved the pristine helium content when globally, OIBs and continental basalts show constanly different degrees of degassing (e.g., Moreira and Kurz, 2013; Kurz et al., 2009). It is worth noting that these two last simulations cannot represent a local MORB-type or SCLM source, because expected ^{4}He content in MORBs are 2 orders of magnitude lower than those used for these simulations (Moreira and Kurz, 2013).

6. Conclusions

This study highlights the possibility of long-term lithospheric storage of primordial noble gases from past magmatic events. The occurrence of mantle-derived helium in the eastern North America craton, first suggested by Torgersen et al. (1995) and then argued by this study, should be further investigated. Analyses of groundwater around intrusions related to the New England

hotspot, such as the White Mountains, should be carried out to confirm the preservation of this mantle memory. Such analyses would also better constrain the hydrogeology of fractured igneous intrusions, which is still poorly documented and understood. The processes leading to the storage of this mantle memory and to its release into groundwater remain to be identified. Recently, Méjean et al. (2017) showed that the release of helium into groundwater could be episodic and related to tectonic events that increase the local fracturing of the rocks. During these events, the release of mantle helium preserved in high-temperature magmatic mineral phases, such as olivine or clinopyroxene, could be substantial. It is then diluted over time by the progressive recharge of the aquifer by freshwater (containing atmospheric helium) and the local accumulation of radiogenic helium. This study suggests that groundwater could preserve a record of mantle helium on a timescale of hundreds of millions of years, and may even provide a more faithful record of the primary signature compared to the magmatic rocks from which the He is ultimately derived.

Acknowledgments

The authors wish to thank Ray Burgess (Un. Manchester), an anonymous reviewer and handling editor F. Moynier for their careful reviews which greatly improved this manuscript. Thoughtful discussions and suggestions with R. Stevenson (GEOTOP) and members of ERC ARCHEIS (Toulouse) were appreciated. D. Graham (OSU) is thanked for giving access to his large noble gas database on MORBs and OIBs. The authors thank the Quebec Ministry of Environment, the Quebec Research Fund ("Fonds de recherche du Quebec - Nature et Technologies"), the Bécancour River Watershed Organization ("organisme de bassin versant COBAVER-VS "), and the municipalities that contributed funding to this research (MRC of Vaudreuil-Soulanges). PM and

LD fellowships were funded by a NSERC Discovery Grant (RGPIN-2015-05378) and a FRQNT project (2010-HO-136990) to DLP.

REFERENCES

Abedini, A.A., Hurwitz, S., Evans, W.C., 2006. USGS-NoGaDat - A global dataset of noble gas concentrations and their isotopic ratios in volcanic systems, Data Series, Reston, VA.

Allègre, C.J., Moreira, M., Staudacher, T., 1995. $^{4}He/^{3}He$ dispersion and mantle convection. Geophys. Res. Lett. 22, 2325-2328.

Andrews, J.N., Kay, R.L.F., 1982. Natural production of tritium in permeable rocks. Nature 298, 361-363.

Beaudry, C., Lefebvre, R., Rivard, C., Cloutier, V., 2018. Conceptual model of regional groundwater flow based on hydrogeochemistry (Montérégie Est, Québec, Canada). Canadian Water Resour. J. 43, 152-172.

Benson, B.B., Krause Jr., D., 1980. Isotopic fractionation of helium during solution: A probe for the liquid state. J. Sol. Chem. 9, 895-909.

Castro, M.C., 2004. Helium sources in passive margin aquifers—new evidence for a significant mantle ^{3}He source in aquifers with unexpectedly low in situ $^{3}He/^{4}He$ production. Earth Planet. Sci. Lett. 222, 897–913.

Castro, M.C., Ma, L., Hall, C.M., 2009. A primordial, solar He–Ne signature in crustal fluids of a stable continental region. Earth Planet. Sci. Lett. 279, 174-184.

Chen, W., Simonetti, A., 2013. In-situ determination of major and trace elements in calcite and apatite, and U–Pb ages of apatite from the Oka carbonatite complex: Insights into a complex crystallization history. Chem. Geol. 353, 151-172.

Chen, W., Simonetti, A., 2015. Isotopic (Pb, Sr, Nd, C, O) evidence for plume-related sampling of an ancient, depleted mantle reservoir. Lithos 216–217, 81-92.

Crough, S., 1981. Mesozoic hotspot epeirogeny in eastern North America. Geology 9, 2-6.

Dixon, J.E., Clague, D.A., 2001. Volatiles in basaltic glasses from Loihi Seamount, Hawaii: evidence for a relatively dry plume component. J. Petrol. 42, 627–654.

Eby, G.N., 1985. Age relations, chemistry, and petrogenesis of mafic alkaline dikes from the Monteregian Hills and younger White Mountain igneous provinces. Can. J. Earth Sci. 22, 1103-1111.

Eby, G.N., 1987. The Monteregian Hills and White Mountain alkaline igneous provinces, eastern North America. Geol. Soc. London, Spec. Publ. 30, 433-446.

Faure, S., Tremblay, A., Angelier, J., 1996. State of intraplate stress and tectonism of northeastern America since Cretaceous times, with particular emphasis on the New England-Quebec igneous province. Tectonophysics 255, 111-134.

Foland, K., Gilbert, L.A., Sebring, C.A., Jiang-Feng, C., 1986. $^{40}Ar/^{39}Ar$ ages for plutons of the Monteregian Hills, Quebec: Evidence for a single episode of Cretaceous magmatism. Geol. Soc. Am. Bull. 97, 966-974.

Gautheron, C., Moreira, M., 2002. Helium signature of the subcontinental lithospheric mantle. Earth Planet. Sci. Lett. 199, 39-47.

Gold, D.P., 1966. The minerals of the Oka carbonatite and alkaline complex, Oka, Quebec. Mineral. Soc. of India IMA Volume, 109-125.

Gonnermann, H.M., Mukhopadhyay, S., 2007. Non-equilibrium degassing and a primordial source for helium in ocean-island volcanism. Nature 449, 1037–1040.

Graham, D.W., 2002. Noble gas isotope geochemistry of mid-ocean ridge and ocean island basalts: Characterization of mantle source reservoirs. Rev. Min. Geochem. 47, 247-317.

Harnois, L., Mineau, R., Morency, M., 1990. Rare-earth element geochemistry of alnoitic Cretaceous rocks and ultramafic xenoliths from Île Bizard (Québec, Canada). Chem. Geol. 85, 135-145.

Harnois, L., Mineau, R., 1991. Geochemistry of the Île Cadieux monticellite alnöite, Quebec, Canada. Can. J. Earth Sci. 28, 1050-1057.

Harðardóttir, S., Halldórsson, S.A., Hilton, D.R., 2018. Spatial distribution of helium isotopes in Icelandic geothermal fluids and volcanic materials with implications for location, upwelling and evolution of the Icelandic mantle plume. Chem. Geol. 480, 12-27.

Heaton, T., Vogel, J., 1981. “Excess air” in groundwater. J. Hydrol. 50, 201-216.

Hopp, J., Trieloff, M., 2008. Helium deficit in high-$^{3}He/^{4}He$ parent magmas: Predegassing fractionation, not a "helium paradox". Geochem. Geophys. Geosyst. 9, Q03009, doi:10.1029/2007GC001833.

Kagoshima, T., Takahata, N., Jung, J., Amakawa, H., Kumagai, H., Sano, Y., 2012. Estimation of sulfur, fluorine, chlorine and bromine fluxes at Mid Ocean Ridges using a new experimental crushing and extraction method. Geochem. J. 46, e21-e26.

Kennedy, B.M., van Soest, M.C., 2007. Flow of mantle fluids through the ductile lower crust: Helium isotope trends. Science 318, 1433-1436.

Kurz, M.D., Jenkins, W.J., Hart, S.R., 1982. Helium isotopic systematics of oceanic islands and mantle heterogeneity. Nature 297, 43-47.

Kurz, M.D., Curtice, J., Fornari, D., Geist, D., Moreira, M., 2009. Primitive neon from the center of the Galápagos hotspot. Earth Planet. Sci. Lett. 286, 23-34.

Lafarge, T., Possolo, A., 2015. The NIST Uncertainty Machine. NCSLI Measure J Meas. Sci. 10, 20-27.

Lamontagne, M., 2002. An overview of some significant eastern Canadian earthquakes and their impacts on the geological environment, buildings, and the public. Nat. Hazards 26, 55-67.

Larocque, M., Meyzonnat, G., Barbecot, F., Pinti, D., Gagné, S., Barnetche, D., Ouellet, M., Graveline, M., 2015. Projet de connaissance des eaux souterraines de la zone de Vaudreuil-Soulanges. Rapport final présenté au Ministère du Développement durable, de l'Environnement, de la Faune et des Parcs (203pp.) (in French).

Lee, H., Kim, H., Kagoshima, T., Park, J.-O., Takahata, N., Sano, Y., 2019. Mantle degassing along strike-slip faults in the Southeastern Korean Peninsula. Sci. Rep. 9, 15334.

Malka, E., Stevenson, R.K., David, J., 2000. Sm-Nd geochemistry and U-Pb geochronology of the Mont Rigaud stock, Quebec, Canada: a late magmatic event associated with the formation of the Iapetus rift. J. Geol. 108, 569-583.

Marty, B., Torgersen, T., Meynier, V., O'Nions, R.K., Marsily, G., 1993. Helium isotope fluxes and groundwater ages in the Dogger Aquifer, Paris Basin. Water Resour. Res. 29, 1025-1035.

Matsuda, J., Matsumoto, T., Sumino, H., Nagao, K., Yamamoto, J., Miura, Y., Kaneoka, I., Takahata, N., Sano, Y., 2002. The $^{3}He/^{4}He$ ratio of the new internal He Standard of Japan (HESJ). Geochem. J. 36, 191-195.

McHone, J.G., 1996. Broad-terrane Jurassic flood basalts across northeastern North America. Geology 24, 319-322.

Méjean, P., 2016. Étude de la circulation des eaux souterraines des basses Terres du Saint-Laurent: approche par les isotopes de l'hélium et de l'uranium. PhD thesis, Université du Québec à Montréal, Montréal, p. 203 (in French).

Méjean, P., Pinti, D.L., Ghaleb, B., Larocque, M., 2017. Fracturing-induced release of radiogenic ^{4}He and ^{234}U into groundwater during the last deglaciation: An alternative source to crustal helium fluxes in periglacial aquifers. Water Resour. Res. 53, 5677-5689.

Moreira M.A., Kurz M.D., 2013. Noble gases as tracers of mantle processes and magmatic degassing, in: Burnard P. (Ed.) The noble gases as geochemical tracers. Advances in Isotope Geochemistry. Springer Berlin Heidelberg, pp. 371-391.

Pinti, D.L., Béland-Otis, C., Tremblay, A., Castro, M.C., Hall, C.M., Marcil, J.-S., Lavoie, J.-Y., Lapointe, R., 2011. Fossil brines preserved in the St-Lawrence Lowlands, Québec, Canada as revealed by their chemistry and noble gas isotopes. Geochim. Cosmochim. Acta 75, 4228-4243.

Pinti, D.L., Retailleau, S., Barnetche, D., Moreira, F., Moritz, A.M., Larocque, M., Gélinas, Y., Lefebvre, R., Hélie, J.-.F., Valadez, A., 2014. ^{222}Rn activity in groundwater of the St. Lawrence Lowlands, Quebec, eastern Canada: Relation with local geology and health hazard. J. Environm. Radioact. 136, 206-217.

Porcelli, D., Elliott, T., 2008. The evolution of He Isotopes in the convecting mantle and the preservation of high ^{3}He/^{4}He ratios. Earth Planet. Sci. Lett. 269, 175-185.

Roulleau, E., Pinti, D.L., Stevenson, R.K., Takahata, N., Sano, Y., Pitre, F., 2012. N, Ar and Pb isotopic co-variations in magmatic minerals: Discriminating fractionation processes from magmatic sources in Monteregian Hills, Québec, Canada. Chem. Geol. 326–327, 123-131.

Roulleau, E., Stevenson, R., 2013. Geochemical and isotopic (Nd–Sr–Hf–Pb) evidence for a lithospheric mantle source in the formation of the alkaline Monteregian Province (Quebec). Can. J. Earth Sci. 50, 650-666.

Saby, M., Larocque, M., Pinti, D.L., Barbecot, F., Sano, Y., Castro, M.C., 2016. Linking groundwater quality to residence times and regional geology in the St. Lawrence Lowlands, southern Quebec, Canada. Appl. Geochem. 65, 1-13.

Sano, Y., Marty, B., Burnard, P., 2013. Noble gases in the atmosphere, in: Burnard, P. (Ed.), The Noble Gases as Geochemical Tracers. Springer Berlin Heidelberg, pp. 17-31.

Sasada, T., Hiyagon, H., Bell, K., Ebihara, M., 1997. Mantle-derived noble gases in carbonatites. Geochim. Cosmochim. Acta 61, 4219-4228.

Sleep, N.H., 1990. Monteregian hotspot track: A long-lived mantle plume. J. Geophys. Res. Solid Earth 95, 21983-21990.

Stuart, F.M., Lass-Evans, S., Fitton, J.G., Ellam, R.M., 2003. High $^{3}He/^{4}He$ ratios in picritic basalts from Baffin Island and the role of a mixed reservoir in mantle plumes. Nature 424, 57-59.

Tolstikhin, I.N., Lehmann, B.E., Loosli, H.H., Gautschi, A., 1996. Helium and argon isotopes in rocks, minerals, and related groundwaters: A case study in northern Switzerland. Geochim. Cosmochim. Acta 60, 1497-1514.

Torgersen, T., 1993. Defining the role of magmatism in extensional tectonics: Helium 3 fluxes in extensional basins. J. Geophys. Res.: Solid Earth 98, 16257-16269.

Torgersen, T., Jenkins, W., 1982. Helium isotopes in geothermal systems: Iceland, the geysers, raft river and steamboat springs. Geochim. Cosmochim. Acta 46, 739-748.

Torgersen, T., Drenkard, S., Stute, M., Schlosser, P., Shapiro, A., 1995. Mantle helium in ground waters of eastern North America: Time and space constraints on sources. Geology 23, 675-678.

Tremblay, A., Roden-Tice, M.K., Brandt, J.A., Megan, T.W., 2013. Mesozoic fault reactivation along the St. Lawrence rift system, eastern Canada: Thermochronologic evidence from apatite fission-track dating. GSA Bull. 125, 794-810.

Trieloff, M., Kunz, J., Clague, D.A., Harrison, D., Allègre, C.J., 2000. The nature of pristine noble gases in mantle plumes. Science 288, 1036-1038.

Vautour, G., Pinti, D.L., Méjean, P., Saby, M., Meyzonnat, G., Larocque, M., Castro, M.C., Hall, C.M., Boucher, C., Roulleau, E., Barbecot, F., Takahata, N., Sano, Y., 2015. $^{3}H/^{3}He$, ^{14}C and (U–Th)/He groundwater ages in the St. Lawrence Lowlands, Quebec, Eastern Canada. Chem. Geol. 413, 94-106.

Weise, S., Moser, H., 1987. Groundwater dating with helium isotopes, in: Isotope techniques in water resources development. International Atomic Energy Agency (IAEA), pp. 105-126.

Figure Captions

Figure 1. Map of the St. Lawrence Lowlands, including the study area of the Vaudreuil-Soulanges watershed (VS) and the intrusions of the Cretaceous Monteregian Hills (MH). The Bécancour watershed (BEC) and the Nicolet and lower Saint-Francois River watershed (NSF) are also indicated. The percentage of mantle helium (f_{mtl}%) measured in each watershed is provided.

Figure 2. a) Map of the sampled groundwater and rocks in the VS watershed, with outcrops of the Cretaceous Oka carbonatite complex and the Île Cadieux alnoïte indicated, together with the Grenvillian Mount Rigaud. b) Map of the sampled groundwater and rocks of the Monteregian Hills.

Figure 3. Distribution of R/Ra values measured in bulk rocks and mineral separates from Monteregian Hills intrusions by Sasada et al. (1997) and in this study. The range of mantle-derived $^{3}He/^{4}He$ measured in groundwater of the St. Lawrence Lowlands basin is also reported for comparison.

Figure 4. (a) Theoretical Weise-type diagram showing the main helium sources, namely the atmosphere, the crust and the mantle, and how the helium isotopic and elemental compositions vary by adding tritiogenic He (light blue arrow), crustal He (yellow arrow), and mantle He (orange arrow) to an atmospheric helium source. A mixing line between a hypothetical tritiogenic helium end-member and sample WSB1 is reported. The intercept of this mixing line with the Y-axis gives the fraction of mantle He in the mixture. (b) Weise diagram of the measured helium ratios. The black line represents mixing between water at recharge (R_{eq}) with water having accumulated crustal radiogenic helium (R_{rad}). Dashed lines through samples represent mixing between modern water of

different initial tritium contents mixed with water containing terrigenic helium (mantle and crustal helium).

Figure 5. Probability distributions of the initial $^3He/^4He$ ratio (R_{mtl}/Ra; Eqn. 6) of the emplaced magma source (alnoïte in the Vadreuil-Soulanges (VS) area and gabbro-sienitic for the Monteregian Hills (MH)), obtained from the Monte Carlo method. These distributions are plotted against the frequency distribution of the R/Ra measured in 401 OIB glasses (data from Abedini et al., 2006). SD = standard deviation (1σ); MAD= mean absolute deviation.

Figure 6. Evolution curves (and uncertainty envelope) of the (R_{mtl}/Ra) as a function of time elapsed since the emplacement of the alnöite intrusions (a) in the VS region 110±3.5 Ma; and (b) in the sampled Monteregian Hills (124 Ma), as calculated by Monte Carlo simulations.

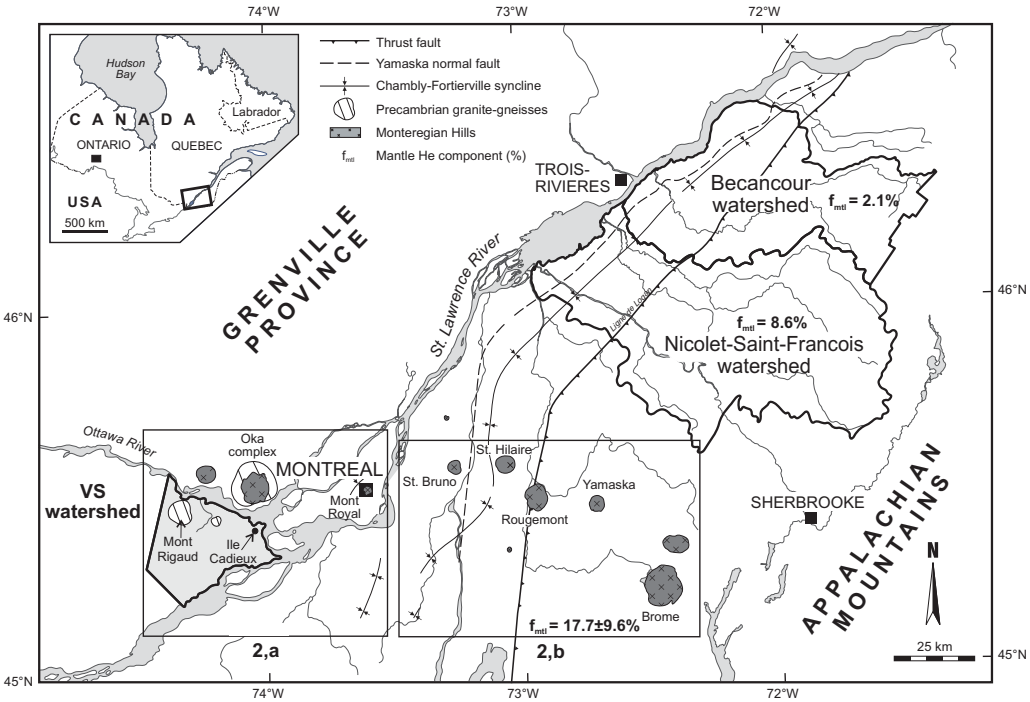

Figure 1
EPSL-D-19-01096R1

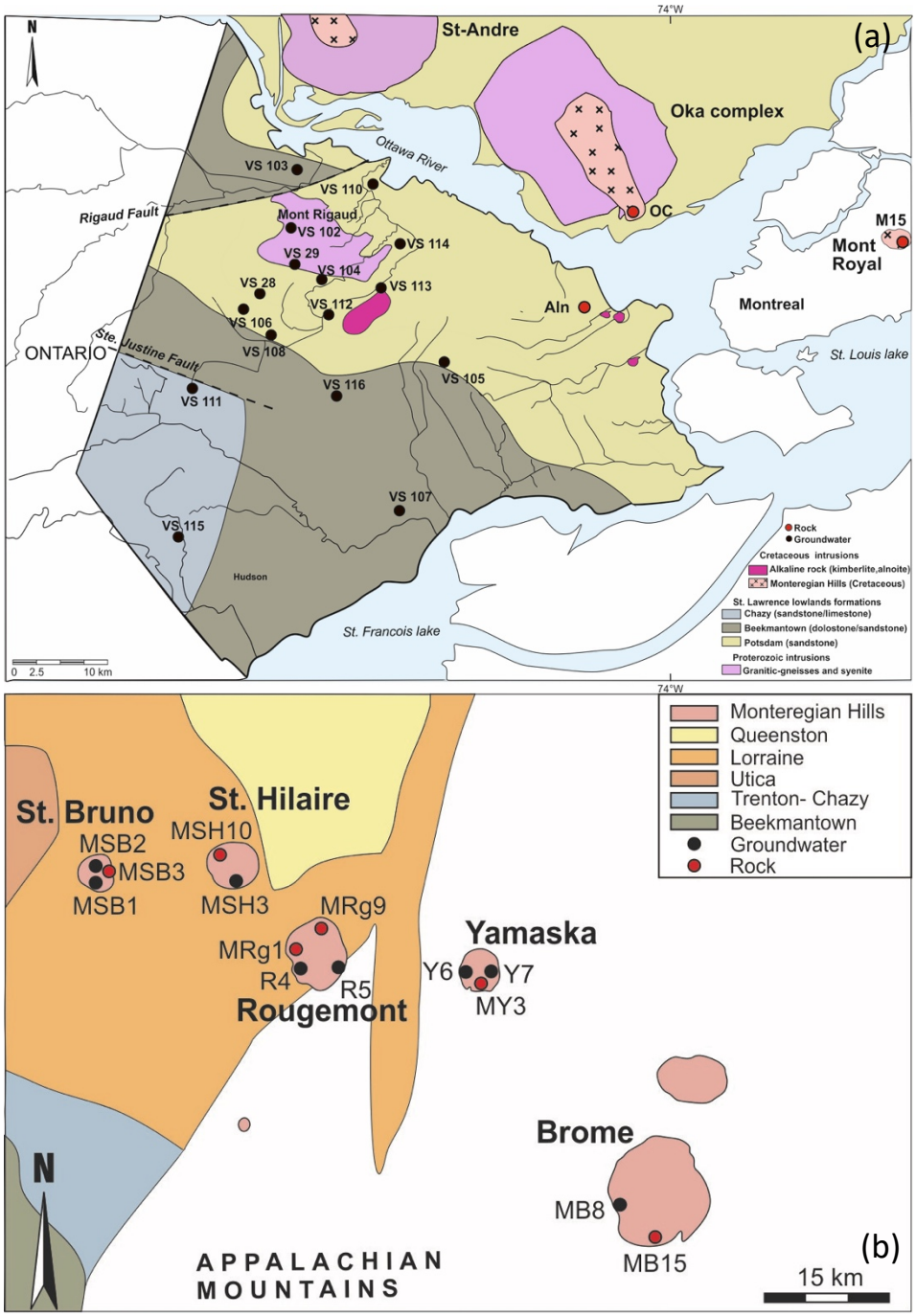

Figure 2 a,b
EPSL-D-19-01096R1

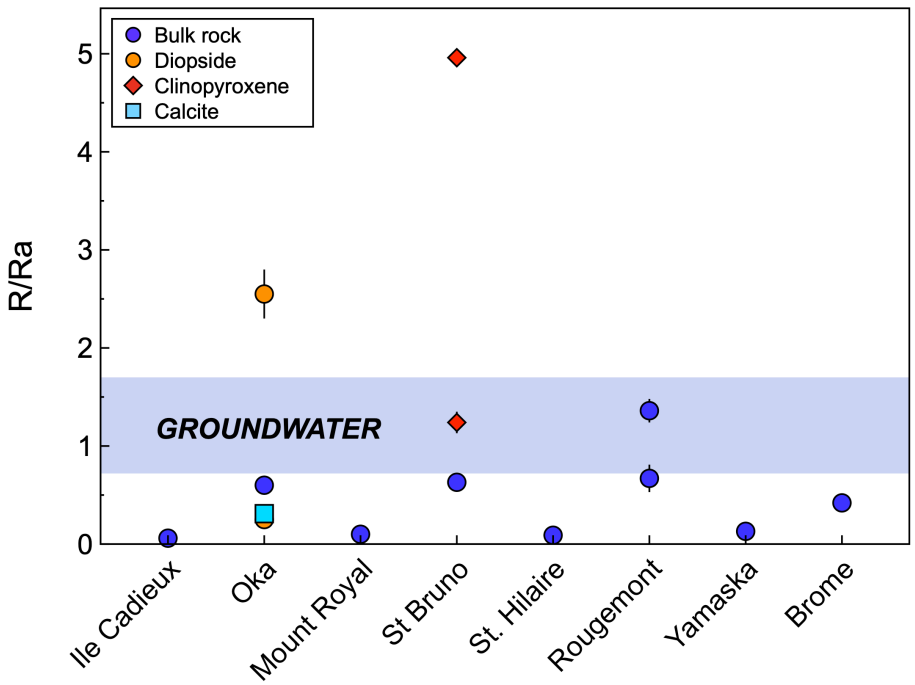

Figure 3
EPSL-D-19-01096R1

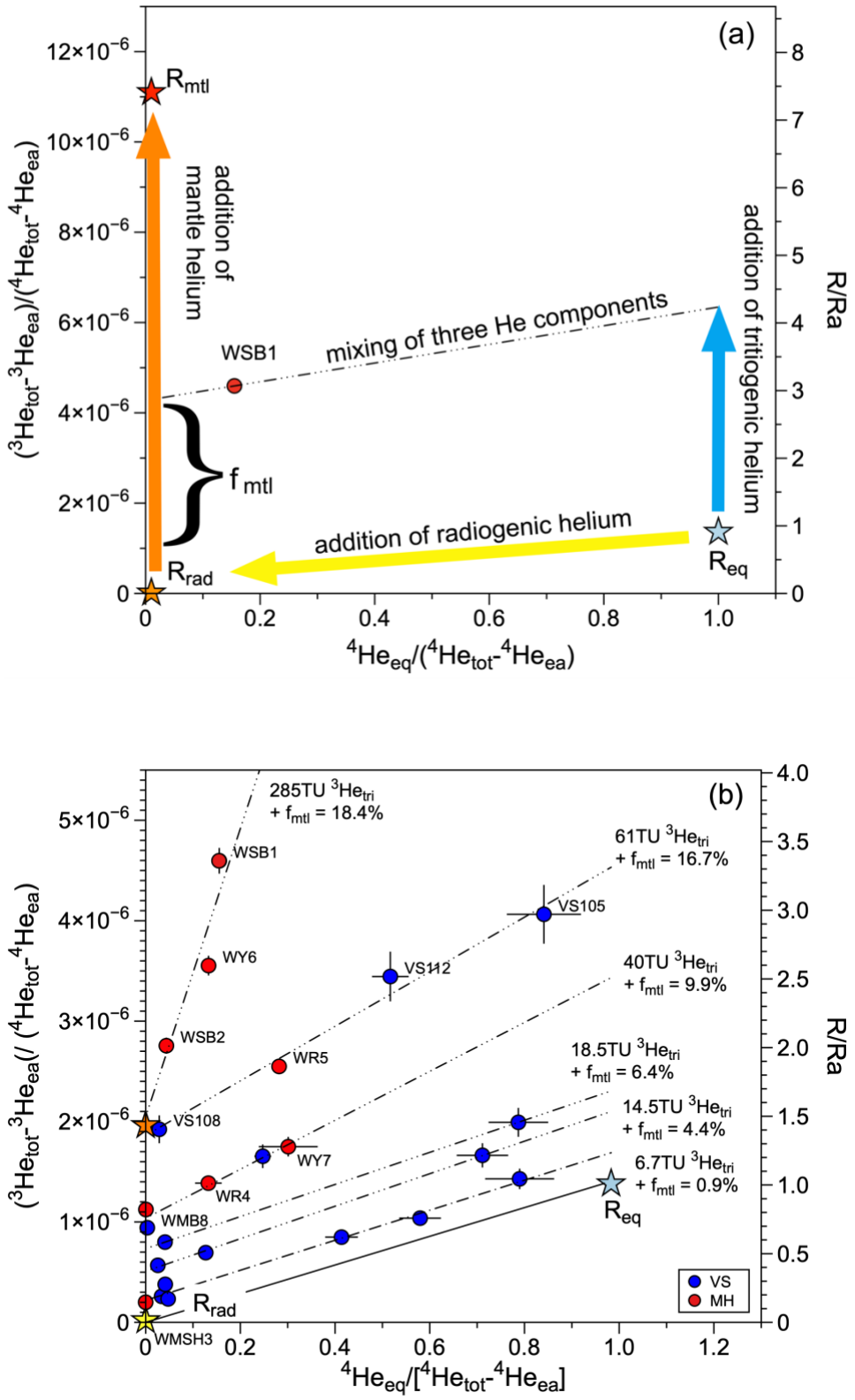
(a)
R_{mtl}
addition of mantle helium
mixing of three He components
WSB1
f_{mtl}
addition of radiogenic helium
addition of tritiogenic helium
R_{rad}
R_{eq}
$(^3He_{tot}-^3He_{ea})/(^4He_{tot}-^4He_{ea})$
R/Ra
$^4He_{eq}/(^4He_{tot}-^4He_{ea})$
(b)
285TU $^3He_{tri}$ + f_{mtl} = 18.4%
61TU $^3He_{tri}$ + f_{mtl} = 16.7%
40TU $^3He_{tri}$ + f_{mtl} = 9.9%
18.5TU $^3He_{tri}$ + f_{mtl} = 6.4%
14.5TU $^3He_{tri}$ + f_{mtl} = 4.4%
6.7TU $^3He_{tri}$ + f_{mtl} = 0.9%
WSB1
WY6
WSB2
VS108
WR5
VS112
VS105
WY7
WR4
WMB8
WMSH3
R_{rad}
R_{eq}
VS
MH
$(^3He_{tot}-^3He_{ea}/(^4He_{tot}-^4He_{ea})$
R/Ra
$^4He_{eq}/[^4He_{tot}-^4He_{ea}]$

Figure 4 a,b

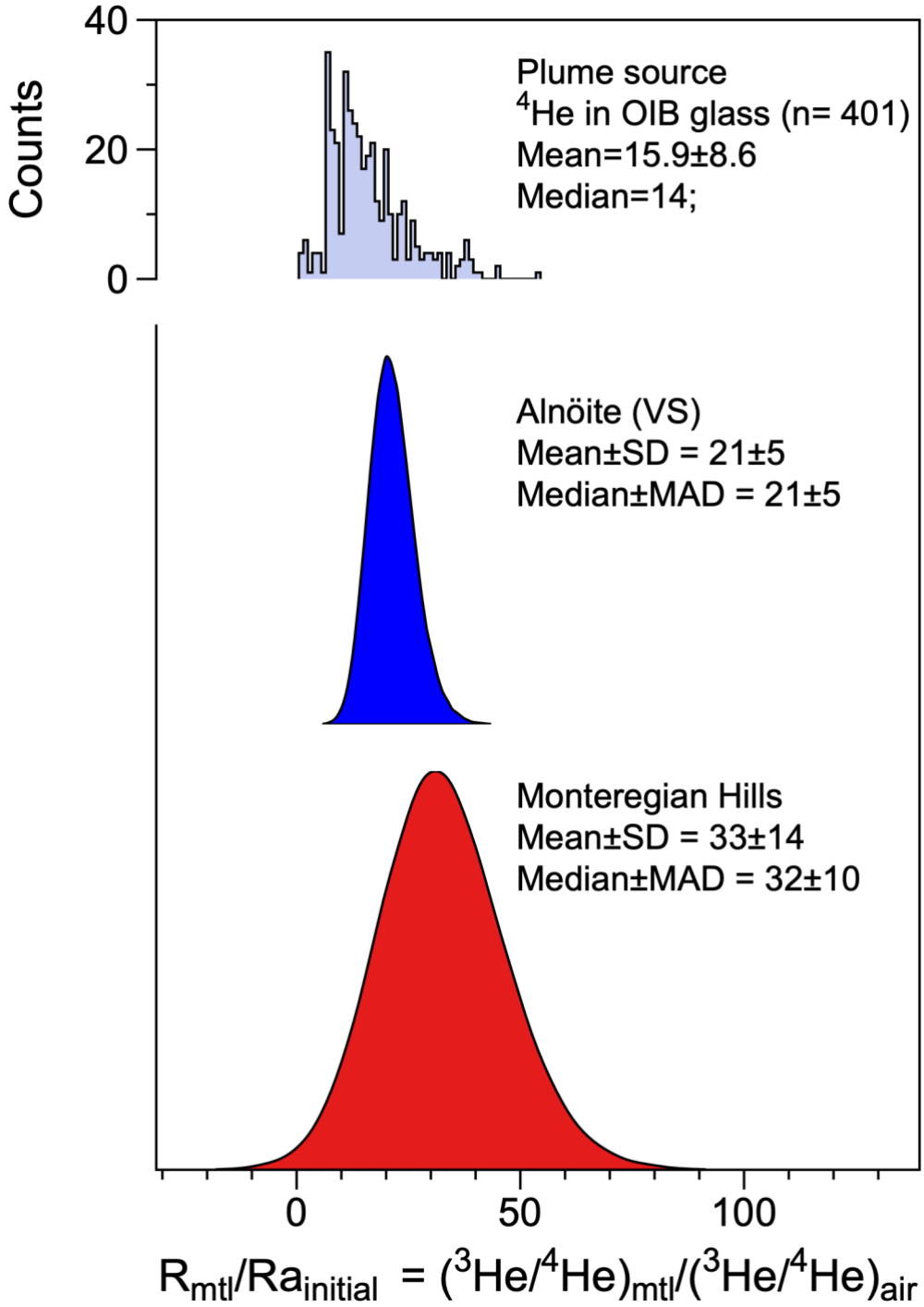

Figure 5
EPSL-D-19-01096R1

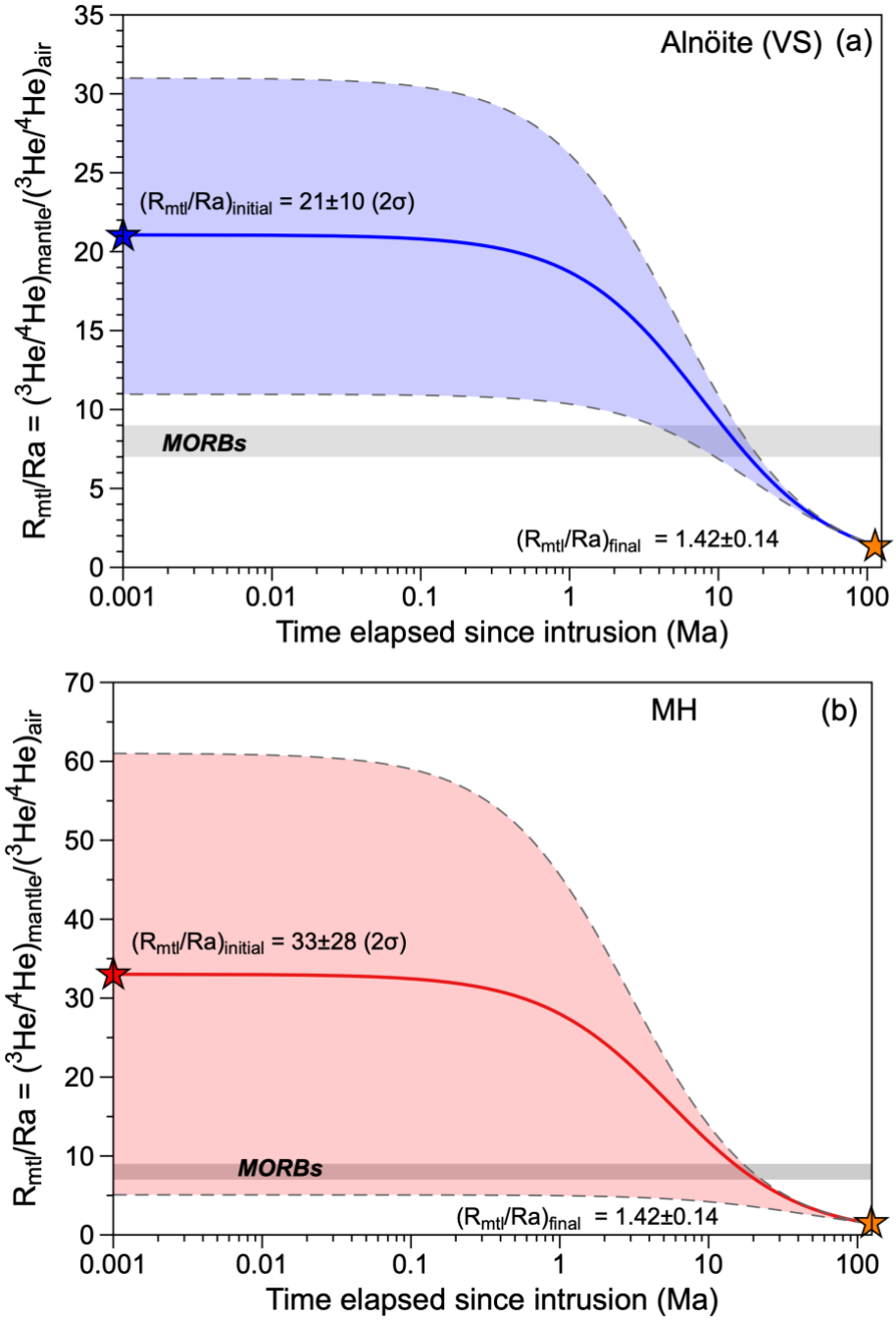

Figure 6 a,b

EPSL-D-19-01096R1

Table 1. Helium and neon elemental and isotopic data of sampled groundwater.

Sample	Type of well	Location	Latitude	Longitude	^{4}He	±	^{20}Ne	±	R/Ra	±	$^{4}He/^{20}Ne$	±	ΔNe%
			UTM NAD83		$cm^3STP/g \times 10^{-8}$		$cm^3STP/g \times 10^{-7}$						(ea)
VS102	Municipal	Vaudreuil-Soulanges	-74.31279	45.44997	9.28	4.64	2.87	0.14	1.02	0.01	0.32	0.16	54.48
VS103	Municipal	Vaudreuil-Soulanges	-74.31123	45.48339	116.10	5.81	2.11	0.10	0.58	0.01	5.51	0.39	12.83
VS104*	Municipal	Vaudreuil-Soulanges	-74.28452	45.42295	6.64	0.33	1.72	0.09	1.20	0.02	0.39	0.03	-8.02
VS105	Observation	Vaudreuil-Soulanges	-74.181861	45.381763	98.81	0.44	2.83	0.14	2.23	0.03	0.31	0.02	51.34
VS106	Observation	Vaudreuil-Soulanges	-74.349212	45.401767	19.46	0.97	1.95	0.10	1.19	0.01	1.00	0.07	4.28
VS107	Observation	Vaudreuil-Soulanges	-74.208624	45.296467	7.46	0.37	2.28	0.11	1.35	0.02	0.33	0.02	21.93
VS108	Private	Vaudreuil-Soulanges	-74.32428	45.3881	166.64	8.33	2.79	0.14	1.38	0.02	5.97	0.42	49.20
VS110	Private	Vaudreuil-Soulanges	-74.25092	45.47927	9.26	0.46	2.17	0.11	0.78	0.01	0.43	0.03	16.04
VS111*	Private	Vaudreuil-Soulanges	-74.38018	45.35587	139.09	6.95	1.75	0.09	0.19	0.01	7.96	0.56	-6.42
VS112	Private	Vaudreuil-Soulanges	-74.2761	45.40286	10.019	0.51	2.16	0.11	2.33	0.03	0.47	0.03	15.51
VS113*	Private	Vaudreuil-Soulanges	-74.23643	45.42119	183.57	9.18	1.53	0.09	0.41	0.01	11.96	0.94	-18.18
VS114*	Private	Vaudreuil-Soulanges	-74.22512	45.44675	1323	68.01	1.79	0.09	0.68	0.01	74.25	5.32	-4.28
VS115	Private	Vaudreuil-Soulanges	-74.38136	45.27199	100	5.03	2.24	0.11	0.18	0.004	4.48	0.32	19.79
VS116	Private	Vaudreuil-Soulanges	-74.26511	45.35669	39.39	1.97	2.54	0.13	0.53	0.01	1.55	0.11	35.83
VS28	Private	Vaudreuil-Soulanges	-74.33418	45.41088	15.19	0.76	3.01	0.15	0.71	0.01	0.50	0.04	60.96
VS29	Private	Vaudreuil-Soulanges	-74.30626	45.42946	139.59	9.41	2.1	0.07	0.28	0.01	6.65	0.50	12.30
WSB1*	Private	MH, St-Bruno	-73.3241974	45.5431257	30.43	0.29	1.76	0.02	3.32	0.08	1.73	0.02	-5.88
WSB2*	Private	MH, St-Bruno	-73.3249577	45.5441935	108.20	1.01	0.67	0.01	1.99	0.05	16.18	0.21	-64.17
WMSH3	Private	MH, St-Hilaire	-73.156288	45.537288	7857827	73675	15780	147	0.15	0.01	49.80	0.66	-
WMSH3 (corrected)					93.12	0.87	1.87	0.02					-
WR4*	Private	MH, Rougemont	-73.080321	45.4633378	35.73	0.33	0.52	0.01	1.00	0.03	6.81	0.09	-72.19
WR5	Private	MH, Rougemont	-73.0336287	45.4605797	17.39	0.16	2.02	0.02	1.81	0.05	0.86	0.01	8.02
WY6	Private	MH, Yamaska	-72.88344	45.46796	38.16	0.36	2.63	0.02	2.46	0.06	1.46	0.02	40.64
WY7*	Private	MH, Yamaska	-72.86829	45.46526	15.72	0.15	0.54	0.01	1.26	0.07	2.92	0.04	-71.12
WMB8	Private	MH, Brome	-72.694374	45.262202	12685	119	1435	13	0.88	0.03	0.88	0.01	-
WMB8 (corrected)					1.65	0.94	1.88	0.02					-

VS = Vadreuil Soulanges watershed; MH = Monteregian Hills

*^{4}He was corrected for degassing when ^{20}Ne is lower than the atmospheric value (solubility of Ne at 9.8°C is 1.87×10^{-7} cm^3STP/g)

ΔNe (%), given as $([Ne]_{measured}/[Ne]_{atmospheric\ equilibrium} - 1 \times 100$, and represents the total amount of excess air

Table 2. Measured helium isotopic composition, calculated helium ratios and He production rates in

Sample	Location	Rock type	Phase	R/Ra	±	[^{4}He]	±
						cm^{3}STP/g x 10^{-5}	
R-Aln	Ile Cadieux	Alnöite	Bulk	0.06	0.02	0.70	0.07
R-OC	Oka Complex	Carbonatite	Bulk	0.60	0.01	1.28	0.12
OKDI*	Oka Complex	Carbonatite	Diopside	0.25	0.07	0.82	0.08
OKDI*	Oka Complex	Carbonatite	Diopside	2.55	0.25	0.13	0.01
OKCA*	Oka Complex	Carbonatite	Calcite	0.31	0.09	1.16	0.12
R-MR15	Mont Royal	Essexite	Bulk	0.10	0.03	0.95	0.09
R-MSB3	St. Bruno	Felsic gabbro	Bulk	0.62	0.06	0.55	0.05
R-MSB3	St. Bruno	Felsic gabbro	Clx-pyroxene	1.23	0.10	0.48	0.04
R-MSB3	St. Bruno	Felsic gabbro	Clx-pyroxene	4.96	0.01	0.07	0.01
R-MB15	Mont Brome	Gabbro	Bulk	0.43	0.03	0.41	0.04
R-MRg1	Mont Rougemont	Banded gabbro	Bulk	0.67	0.13	0.07	0.01
R-MRg9	Mont Rougemont	Gabbro	Bulk	1.36	0.11	0.41	0.04
R-MSH10	Mont St. Hilaire	Gabbro	Bulk	0.09	0.01	2.28	0.22
R-MY3	Mont Yamaska	Gabbro	Bulk	0.13	0.01	1.92	0.19

* Data from Sasada et al. (1997)

**Rin/Ra is the resulting helium isotopic ratio from in situ production of ^{3}He and ^{4}He.

ı Monteregian Hills' rocks and minerals.

[U] ppm	[Th] ppm	[Li] ppm	J^3He $cm^3STP/g_{rock}/y$ r x 10^{-20}	±	J^4He $cm^3STP/g_{rock}/y$ r x 10^{-13}	±	R_{in}/Ra**
3.3	15.4	15	1.78	0.36	8.41	1.68	0.015
9.9	40.9	15	0.63	0.13	23.56	4.71	0.002
n.d.	n.d.	n.d.	n.d.	n.d.	n.d.	n.d.	n.d.
n.d.	n.d.	n.d.	n.d.	n.d.	n.d.	n.d.	n.d.
n.d.	n.d.	n.d.	n.d.	n.d.	n.d.	n.d.	n.d.
4.5	9.6	37	1.58	0.32	8.48	1.7	0.013
3.9	9.4	28	1.04	0.21	7.35	1.5	0.010
n.d.	n.d.	n.d.	n.d.	n.d.	n.d.	n.d.	n.d.
n.d.	n.d.	n.d.	n.d.	n.d.	n.d.	n.d.	n.d.
12.4	20.1	28	2.89	0.58	20.54	4.1	0.010
4.5	8.8	28	1.11	0.22	7.89	1.58	0.010
4.1	9.4	28	1.07	0.21	7.59	1.5	0.010
10.0	19.6	28	2.47	0.50	17.64	3.5	0.010
6.6	17.7	28	1.82	0.36	13.0	2.6	0.010

Table 3. Summary of input and output parameters for Monte Carlo simulations.

Input parameters	units	Alnoite	±	MH	±
J_4He	x 10^{-13} ccSTP/g_{rock}/yr	8.41	1.68	11.78	5.01
$(R_{mtl}/Ra)_{final}$		1.42	0.14	1.42	0.14
^4He initial	x 10^{-6} ccSTP/g	6.7	0.7	6.7	0.7
Age since intrusion	Ma	110.5	3.5	124	1
Output parameter :					
$(R_{mtl}/Ra)_{initial}$	Average*	21	5	33	14
$(R_{mtl}/Ra)_{initial}$	Median**	21	5	32	10

Monte Carlo simulation results after 1 x 10^5 iterations.

* Uncertainty on the avearge value is standard deviation (1σ)

** Uncertainty on the median is the mean absolute deviation (MAD)